Research Article

Preparation and Evaluation of Miconazole Nitrate-Loaded Solid Lipid Nanoparticles for Topical Delivery

Mangesh R. Bhalekar,[1,3] Varsha Pokharkar,[2] Ashwini Madgulkar,[1] Nilam Patil,[1] and Nilkanth Patil[1]

Abstract. The purpose of this study was to prepare miconazole nitrate (MN) loaded solid lipid nanoparticles (MN-SLN) effective for topical delivery of miconazole nitrate. Compritol 888 ATO as lipid, propylene glycol (PG) to increase drug solubility in lipid, tween 80, and glyceryl monostearate were used as the surfactants to stabilize SLN dispersion in the SLN preparation using hot homogenization method. SLN dispersions exhibited average size between 244 and 766 nm. All the dispersions had high entrapment efficiency ranging from 80% to 100%. The MN-SLN dispersion which showed good stability for a period of 1 month was selected. This MN-SLN was characterized for particle size, entrapment efficiency, and X-ray diffraction. The penetration of miconazole nitrate from the gel formulated using selected MN-SLN dispersion as into cadaver skins was evaluated *ex-vivo* using franz diffusion cell. The results of differential scanning calorimetry (DSC) showed that MN was dispersed in SLN in an amorphous state. The MN-SLN formulations could significantly increase the accumulative uptake of MN in skin over the marketed gel and showed a significantly enhanced skin targeting effect. These results indicate that the studied MN-SLN formulation with skin targeting may be a promising carrier for topical delivery of miconazole nitrate.

KEY WORDS: miconazole nitrate; skin targeting; solid lipid nanoparticles; topical delivery.

INTRODUCTION

Targeted drug delivery implies selective and effective localization of pharmacologically active ingredient at pre-selected target in therapeutic concentration, while restricting its access to non-target areas, thus maximizing the effectiveness of the drug. The carrier is one of the most important entities required for successful transportation of the drug. Colloidal drug delivery system is a rapidly developing area that has contributed significantly to the progress in the field of controlled and targeted drug delivery. Colloidal carriers are one of the approaches for the controlled delivery of drugs by the dermal route (1–5).

As a vehicle for controlled release of active substances and targeting to skin layers, nanodisperse systems such as liposomes, nanoemulsions, and lipid nanoparticles are gaining more and more importance. Solid lipid nanoparticles (SLNs) are the new generation of nanoparticulate active substance vehicles and are attracting major attention as novel colloidal drug carriers for topical use. Nanosized lipid vesicles have various advantages, but it overcomes the disadvantages of other colloidal carriers such as liposomes, microemulsion, and

polymeric nanoparticles (6). SLNs were developed at the beginning of the 1990s as an alternative carrier system to emulsions, liposomes, and polymeric nanoparticles. Compared with polymeric nanoparticles, SLNs have lower toxicity because of the absence of solvents in the production process and also relatively low cost of the excipients. SLNs combine their advantages such as controlled release, biodegradability, and protection of active compounds (1,2). Especially, SLN can favor drug penetration into the skin (3,4), maintain a sustained release to avoid systemic absorption (5), act as a UV sunscreen system (4), and reduce irritation (7,8). SLN represents a particulate system, which can be produced with an established technique of high-pressure homogenization, allowing production on industrial scale. This method also protects the incorporated drug against chemical degradation, as there is little or no access for water to enter the inner area core of the lipid particle (1).

Stratum corneum is the main barrier in the percutaneous absorption of topically applied drugs. Small size and relatively narrow size distribution of SLN permit site-specific delivery to the skin (3,9). SLNs have high affinity to the stratum corneum, and therefore an enhanced bioavailability of the encapsulated material to the skin is achieved. SLNs enhance the penetration and transport active substances particularly lipophilic agents and thus intensify the concentration of these agents in the skin (4,10). Recently, the research activities on SLN has gradually focused on the cosmetic and topical product; SLNs as a topical carrier were used for topical

[1] AISSMS College of Pharmacy, Kennedy Road, Pune 411001, India.
[2] Bharati Vidyapeeth University, Poona College of Pharmacy, Erandwane, Pune 411038, India.
[3] To whom correspondence should be addressed. (e-mail: mrb1570@yahoo.com)

delivery of several drugs including clotrimazole, prednicarbate, and betamethasone 17-valerate and SLN was reported to have a skin-targeting potential (7,8,11,12). SLN was found to have a skin targeting which can result in a high accumulation of podophyllotoxin in skin (13). In this work, SLN was used for topical delivery of miconazole nitrate (MN) and the long-term aim is to explore a novel formulation with skin-targeting effect for the treatment of fungal infections. Miconazole nitrate (1H-imidazole, 1-[2-(2, 4 dichlorophenyl)-2-[(2, 4 dichlorophenyl)methoxy]ethyl-,mononitrate) is an imidazole anti-fungal agent, which is clinically administered both in oral and topical formulations. MN is insoluble in water and soluble in methanol, in hot chloroform, and in dimethyl formamide (DMF). MN has a partition coefficient of about 6.25 in octanol–water system. This study investigates the formulation and characterization of SLN on miconazole nitrate. The lipid nanoparticles were incorporated in gels for convenient topical application and were evaluated for *ex vivo* skin penetration.

MATERIALS AND METHODS

Materials

Compritol 888 ATO (glyceryl behenate), Precirol ATO 5 (glycerol palmitostearate), and Emulcire 61 (cetyl alcohol, Ceteth-20, and Steareth-20) were obtained as gift sample from Gattefosse (Colorcon, India). Tween 80, glyceryl monostearate (GMS), propylene glycol (PG), DMF, soya lecithin, and carbopol 940 were provided by Loba Chemie (India). MN was gifted by Glenmark (Washi, Mumbai, India). All other chemicals were of reagent grade and used without further purification.

Partitioning Behavior of Miconazole Nitrate in Various Lipids (14)

Ten milligrams of miconazole nitrate was dispersed in a mixture of melted lipid (1 g) and 1 ml of hot distilled water and shaken for 30 min in a hot water bath. Aqueous phase was separated after cooling by ultracentrifugation and analyzed for drug content.

Preparation of SLN

MN was dispersed in the lipid melt of compritol 888 ATO and GMS; then, PG was added to obtain clear solution.

The dispersion medium (distilled water with Tween 80) was heated to the temperature of 80°C and the hot lipid phase was emulsified in the dispersion medium by high-speed stirring using Ultra-Turrax T 25 (IKA-Werke, Staufen, Germany) at 9,000 rpm for 5 min. This dispersion was then subjected to high-pressure homogenization (HPH) using Nero Soavi S.P.A. (Italy) homogenizer at 500 bars and five cycles. The dispersion thus obtained was allowed to cool to room temperature, forming lipid nanoparticles by recrystallization of the dispersed lipid (15). On the basis of physical stability, formulation of dispersion was further optimized for different percentages of surfactants (Table I).

CHARACTERIZATION OF MN-SLN

Particle Size

The particle size analysis of prepared dispersions was performed using Malvern Mastersizer 2000 (Malvern Instruments, Worcestershire, UK) with beam length 2.40 mm, range lens of 300 RF mm, and at 14.4% obscuration.

Determination of MN Entrapment in SLNs

MN-SLN dispersion was separated by ultracentrifugation (Beckmann instrument, Italy) at 35,000 rpm corresponding to approximately $116,000 \times g$. The collected samples were added in chloroform and warmed to dissolve completely, and then it was extracted with DMF which dissolved only miconazole nitrate.

The solution was filtered and diluted with methanol and miconazole nitrate content was determined spectrophotometrically. Percentage of entrapment efficiency (%EE) was calculated by the following formula

$$\% \ EE = \frac{\text{The amount of entrapped drug in SLN}}{\text{The amount of entrapped drug in SLN and free drug in dispersion}} \times 100$$

Determination of Unentrapped Miconazole Nitrate

Free drug expressed as the percentage of the added drug remained unentrapped in supernatant liquid, which was obtained after ultracentrifugation. Each estimation was repeated three times.

Table I. SLN Dispersions of Miconazole Nitrate with Different Percentage of Lipid and Surfactants

Sample	MN (%)	Comp. 888 (%)	T. 80 (%)	GMS (%)	PG (%)	Water (ml)
A	1	5	2.5	1.5	2	88
B	1	5	1.25	1.5	2	89
C	1	3	2.5	1.5	2	90
D	1	3	1.25	1.5	2	91
E	1	5	1.5	1.5	1	89
F	1	3	2.5	1.5	1	91

Comp. 888 compritol 888 ATO, *T. 80* Tween 80, *GMS* glyceryl monostearate, *PG* propylene glycol

Table II. Mean Percent Miconazole Nitrate Entrapped in SLNs and Particle Size

Sample	Entrapment efficiency (%)±SD	Particle size (nm)±SD
A	94±3.60	261±2.67
B	94±3.54	720±3.41
C	70±4.04	460±4.84
D	72±2.64	730±4.86
E	94±3.26	766±3.69
F	68±2.62	244±3.16

Stability of the Miconazole Nitrate-Loaded SLN

The chemical and physical stability of MN-SLN dispersion was evaluated at 2–8°C for 1 month via clarity, particle size, and drug content.

DSC Measurements

Differential scanning calorimetry (DSC) on MN, MN-SLN, and compritol 888 ATO was performed by Mettler-Toledo DSC 821^e (Columbus, OH, USA) instrument, and an empty standard aluminum pan was used as reference. DSC scans were recorded at heating rate of 10°C/min in temperature range of 30–250°C.

X-ray Diffraction

X-ray scattering measurements were carried out with a Philips PAN analytical expert PRO X-ray diffractometer 1780 (Netherlands).

FTIR Studies

A Jasco Fourier transform infrared (FTIR) spectrophotometer (Jasco FTIR- 401, Japan) was used for infrared analysis of samples. About 1–2 mg of sample were mixed with dry potassium bromide and the samples were examined at transmission mode over wavenumber range of 4,000 to 400 cm^{-1}. FTIR studies were carried out on pure compritol 888 ATO, MN, and MN-SLN.

PREPARATION AND EVALUATION OF MICONAZOLE NITRATE GELS

Gels containing MN-SLN were prepared with different percent of carbopol 940 (0.3–1.0%) and analyzed as described below. Gel containing plain miconazole nitrate (marketed formulation) was acquired from the market. MN-SLN gels were prepared as required quantity of carbopol 940 was weighed and dispersed in small quantity of distilled water to prepare aqueous dispersion. The dispersion was allowed to hydrate for 4 to 5 h. Glycerol (10% *w/w*) was added subsequently to the aqueous dispersion and the pellet obtained from centrifuged MN-SLN dispersion equivalent to 2 g was incorporated to prepare gel of 2% (16,17). Triethanolamine was added to the above dispersion under gentle stirring and the pH was adjusted to 6.0. The gel was allowed to stand overnight to remove entrapped air.

MN-SLN gel (2%) was assayed by dissolving gel in chloroform and sample was analyzed by suitably diluting with methanol.

Small-angle cone and plate rheometers are used to determine the shear stress *versus* shear rate for a variety of formulations. The aim of the present study was to assess the thixotropic behavior of SLN-based semisolid formulations prepared with carbopol 940 as jellifying agent. To gain some insight into the influence of storage temperature and nature of lipid matrix, the shear stress variation was recorded at pre-defined shear rate from 0 to 1,000 s^{-1} for semisolid systems stored at three different temperatures (5°C, 25°C, and 40°C).

Ex Vivo Skin Penetration Studies

Human cadaver skin (HCS) was taken from the abdominal region, after removing hair and subcutaneous fat tissue, punching out a disk of approximately 2.2-cm^2 area. The skin was hydrated for 24 h in the diffusion medium then mounted on the Franz diffusion cell (22-ml capacity with 2.2-cm^2 diffusional surface area). Acetate buffer (pH 5) containing 10% polyethylene glycol 400 served as receptor fluid stirred at 500 rpm using magnetic stirrer. A small quantity (0.1 g) of the gel was applied to the skin surface and temperature of diffusion cell was maintained at 32°C. Serial sampling (0.5 ml) was performed at specified time intervals (1, 2, 3, 4, 5, 6, 7, 8,
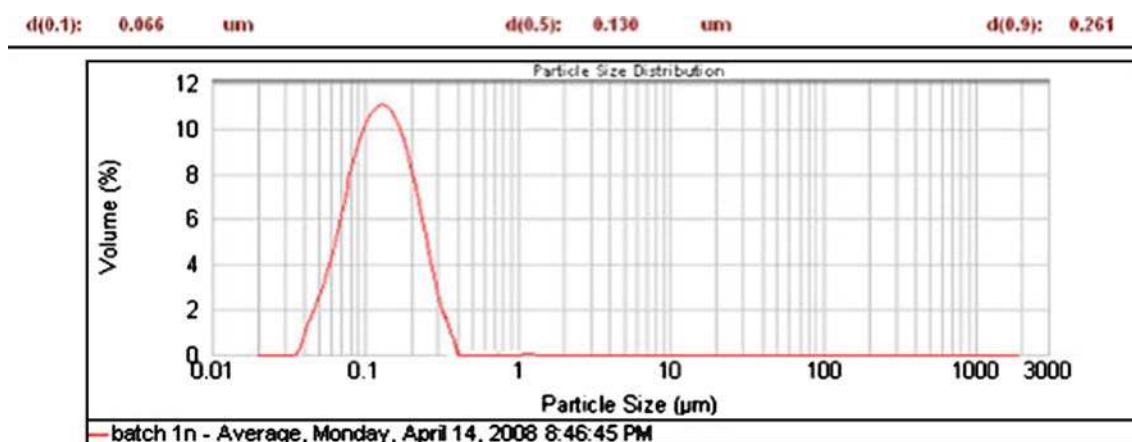

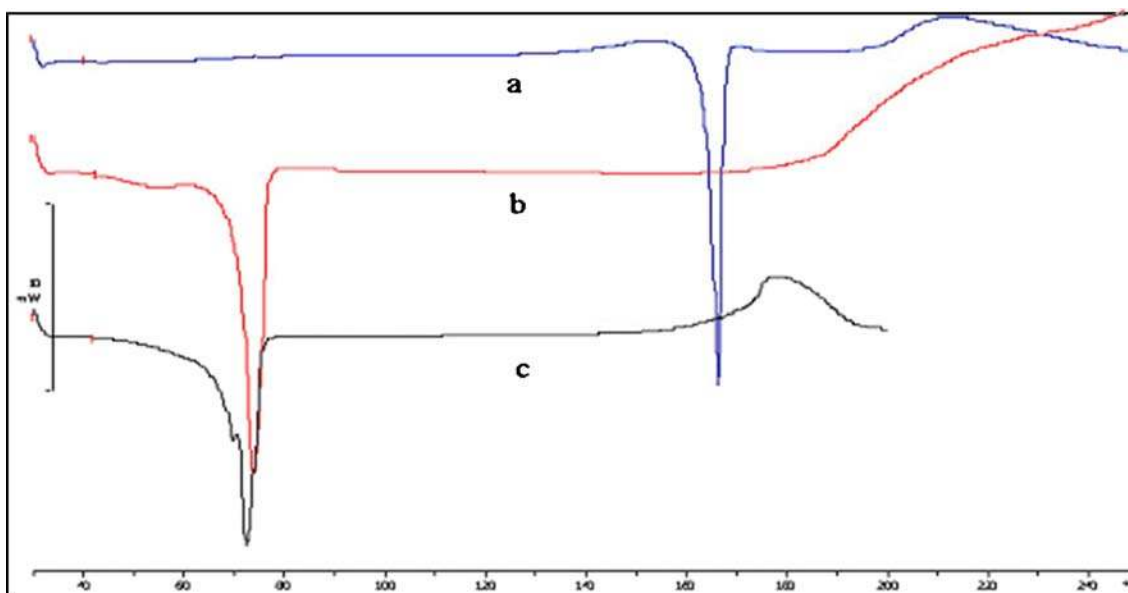**Fig. 1.** Particle size distribution curve of sample A

Fig. 2. Differential scanning thermograms of bulk material of miconazole nitrate (*a*), compritol 888 ATO (*b*), and MN-SLNs (*c*)

10, 12, 18, 24 h) by removing the contents of the receptor compartment and replacing it with the fresh medium. The samples were analyzed using Jasco UV-VIS spectrophotometer at 220 nm and mean cumulative amount diffused Q (mg/cm^2) at each sampling time points was calculated. At the end of 24 h, the skin was cut, homogenized, and extracted, first with methanol and then filtered; the methanolic extract was evaporated and the residue was again extracted with DMF, filtered, diluted with 0.1 N HCl, and analyzed spectrophotometrically at 220 nm.

RESULTS AND DISCUSSION

Partitioning Behavior of Miconazole Nitrate

Calibration curve ($y=0.0547x+0.0444$, $R^2=0.9978$) of miconazole nitrate was used to calculate the concentration

of MN in the aqueous phase. Partition coefficients (ratio of the amount of miconazole nitrate in lipid to the amount of miconazole nitrate in aqueous phase) obtained by analyzing drug content in aqueous phase were 37 ± 2.14, 72.54 ± 1.85, and 46 ± 1.58 for Emulcire 61, compritol 888 ATO, and Precirol ATO 5, respectively. Compritol 888 ATO in which miconazole nitrate exhibited higher partition coefficient was selected for preparation of SLN.

Preparation of Solid Lipid Nanoparticle Dispersion

Solid lipid nanoparticle dispersion of MN was successfully prepared by melt homogenization method. Three homogenization cycles at pressure of 500 bars provides less dispersion energy per unit lipid, thus leading to larger particle sizes (10). To compensate for this, a higher number of homogenization cycles (five cycles) needs to be applied to
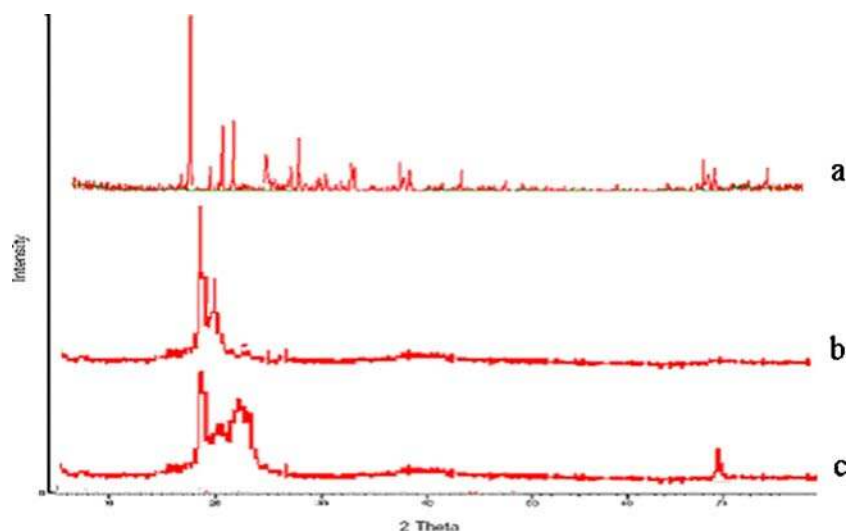

Fig. 3. X-ray diffractograms of bulk material of miconazole nitrate (*a*), compritol 888 ATO (*b*), and MN-SLNs (*c*)
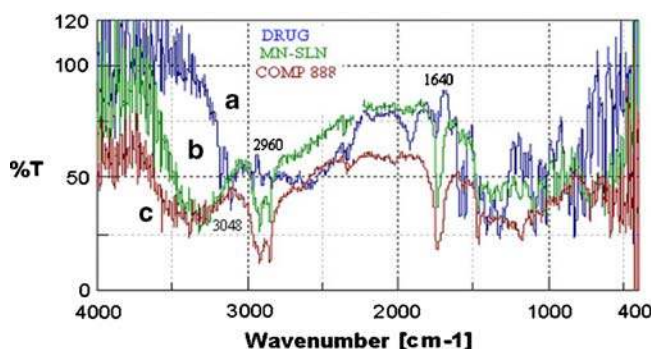
Fig. 4. Fourier transform infrared spectrums: (*a*) bulk material of miconazole nitrate, (*b*) MN-loaded lipid nanoparticles, and (*c*) Bulk material of compritol 888 ATO

provide high dispersion energy per unit lipid resulting in small sizes of SLN. The nanoparticulate dispersion was white in color and odorless and did not show sedimentation even after centrifugation at 2,000 rpm for 30 min.

Particle Size Analysis

The *d* (90) for nanoparticulate dispersions determined using Malvern Mastersizer showed size raging from 244 to 766 nm (Table II). The effect of Tween 80 concentration on the particle size can be seen from particle size of samples A, F, and C (261, 244, and 460 nm, respectively); samples B, D, and E show particle size between 700 and 750 nm with less surfactant concentration (1.25%). Particle size distribution of sample A is shown in Fig 1.

Percentage of Entrapment Efficiency

A high amount of drug could be incorporated in nano-particle dispersion. Such high incorporation was possible because of lipid solubility of MN and use of PG as co-solvent. The %EE of different formulations prepared is shown as in Table II. It can be seen that lipids show positive influence on entrapment efficiency as samples A, B, and E show %EE of

about 94% while samples C, D, and F show less %EE (about 70%). Sample A was selected as optimized SLN dispersion since it showed less particle size and high entrapment efficiency as compared to other dispersions.

Differential Scanning Calorimetry (18,19)

DSC is a highly useful means of detecting drug–excipient incompatibility in the formulation. Compritol 888 ATO alone and in formulation was studied using DSC. For the bulk material of compritol 888 ATO, the melting process took place with maximum peak at 71.97°C and MN shows peak at 168°C shown in Fig. 2. DSC thermogram of MN-SLN showed an endotherm at 70°C, which can be attributed to melting of compritol 888 ATO in SLN.

The peak of compritol 888 ATO in formulation shows a shift to the lower temperature side. This could be due to reduction in particle size and increase in surface area leading to decrease in melting enthalpy as compared with heat flow through larger crystals, which require more time. The higher melting enthalpy value suggests higher ordered lattice ar-rangement. For the less-ordered crystal/amorphous state, the melting of the substance requires less energy than the perfect crystalline substance, which needs to overcome lattice force. Decrease in melting point and transformation of a sharp peak to a peak with shoulder associated with the numerous lattice defects and the formation of amorphous regions in which the drug is located. Also shown is a new peak at 200°C due to presence of miconazole nitrate.

X-ray Diffraction

X-ray diffraction data listed in Fig. 3 were in good agreement with results established by DSC measurements. The diffraction pattern of MN exhibits sharp peaks at about 2θ scattered angles, indicating the crystalline nature of MN (20). The characteristic peaks for MN was absent in the SLN XRD pattern suggesting that MN was not in crystalline form in SLN, diffraction pattern of the MN-SLN was broader and much weaker than that of bulk lipid (compritol 888 ATO). It indicated that compritol 888 ATO in MN-SLN was partially recrystallized or less ordered. It was clear that, from MN-SLN, the less-ordered crystals were majority and the amor-
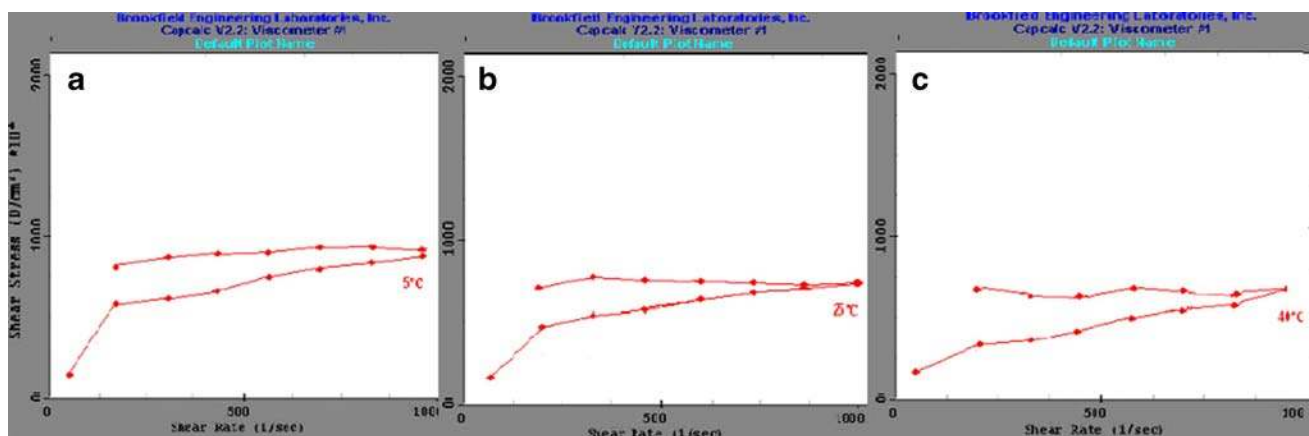

Fig. 5. Thixotropic behavior of gels containing MN-SLNs (**a**) at 5°C, (**b**) at 25°C, and (**c**) at 40°C
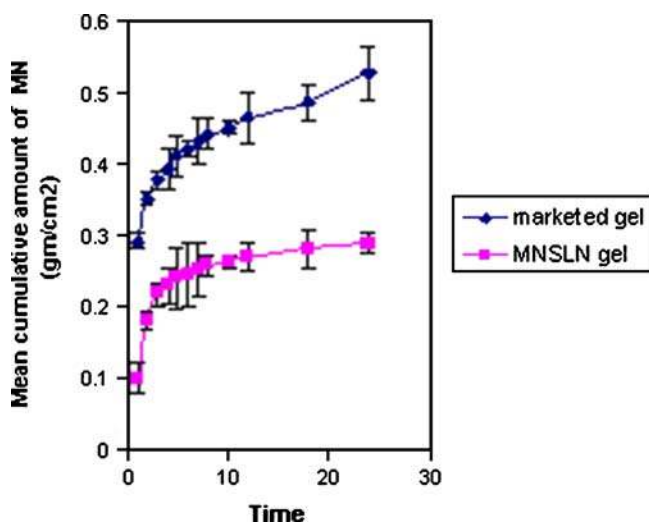
Fig. 6. *Ex-vivo* release of miconazole nitrate from marketed and SLN gels of 2% miconazole nitrate

Table III. Mean Amount of Miconazole Nitrate Deposited into HCS

Test formulation	Human cadaver skin (%) mean (±SD)	Gel (%) mean (±SD)
MN marketed gel	30±2.67	45±3.21
MN-SLN gel	57±1.96	28±2.14

Mean of three determinations (*n*=3)

the number of imperfections in the crystal lattice is reduced thus leading to drug expulsion (10).

phous state would contribute to the higher drug loading capacity as seen previously (13). This confirms that our method of preparation (HPH) and the presence of surfactants did not allow the drug to crystallize.

FTIR

The FTIR spectrum shows characteristic peaks of MN such as aromatic C=N stretching (1,640 cm^{-1}), aliphatic C–H stretching (2,960 cm^{-1}), aromatic C–H stretching (3,048 cm^{-1}). The compritol showed peaks corresponding to C=O stretching (1,635 cm^{-1}) and aliphatic C–H stretching (2,956 cm^{-1}). In the IR spectrum of SLN, peaks corresponding to MN disappear or are buried in the peaks of compritol 888 ATO indicating drug entrapment in lipid matrix as shown in Fig. 4. The miconazole due to high melting point may have precipitated as core and the compritol may have formed the coating around the drug core as suggested from the above data.

Stability Study

After 1 month of refrigerated storage, the SLN dispersion showed little difference in particle size and entrapment efficiency. No obvious change of clarity and degradation was observed. The particle size and entrapment efficiency of sample A stored for 1 month were 280±3.18 nm and 92± 2.69% content. Centrifugation at 3,000 rpm for 30 min also showed that the MN-SLN had a good physical stability. This may imply that the transition of dispersed compritol 888 ATO in SLN dispersion from β' form to stable β form might occur extremely slowly.

Generally, the SLNs are prepared from solid lipids or blends of solid lipids and, after the preparation by hot homogenization technique, the particle crystallizes, at least partially, in higher energy modifications α and β'. During storage, these modifications can transform to the low-energy more-ordered β modification. Due to its high degree of order,

Preparation and Evaluation MN-SLN Gel

Gel of MN-SLN was prepared by using different concentrations of carbopol 940 (0.3–1%) out of which 0.5% concentration showed good consistency. Drug content in gel was 98±0.85% (*n*=3).

The rheological behavior of gel entrapping MN-SLN kept at different temperatures was performed as shown in Fig. 5.

Dispersions of lipid nanoparticles under shear flows experience different types of forces such as hydrodynamic forces (including the viscous drag force and particle–particle interaction through flow field induced by the neighboring particles), colloidal chemical forces (including electrostatic, steric, and London-van der Waals attractive forces), and forces due to gravitational, inertial, electro-viscous, and thermal or molecular collision effects. For the evaluation of these properties, the applied stress, as well as the duration of the stress application, must be previously defined in order to avoid the destruction of the structure, so that measurements can provide information of the inter-molecular and inter-particle forces in the material (21). Small-angle cone and plate rheometers are used to determine the shear stress *versus* shear rate for a variety of formulations (23). This device has the advantage that experimental data, in the form of measured torque and normal force at different rotational speeds, can be converted directly into shear stress and first normal stress functions, using very simple algebraic expres-
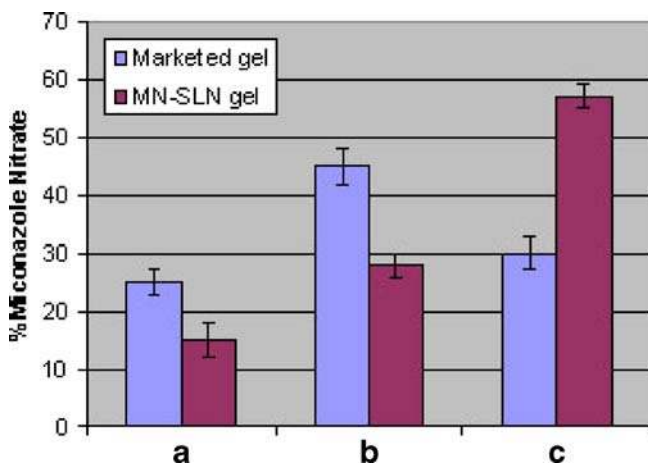

Fig. 7. Comparison of the drug levels from *ex-vivo* skin penetration studies: (*a*) receptor compartment, (*b*) remained on the skin, and (*c*) penetrated in the skin

sions that are independent on the rheological constructive equation. These expressions are based on the small-angle approximation which means that the shear rate and consequently the shear and normal stresses are essentially uniform and known throughout the fluid under test. Knowledge of the rheological properties is very important because the microstructural environmental or mobility, which is responsible for drug diffusion and compatibility, can be indirectly probed using these measurements. Extensive study may lead to the possible employment of rheological parameters and models to optimize topical drug delivery from dermatological formulations. Due to their importance, the rheological properties of carbomer gels (carbopols) have extensively been investigated as a function of concentration, pH, and cross-link density (24,25). Most of the studies use water as the solvent with a few reports about hydroalcoholic system (26). Therefore, exhaustive characterization of the flow behavior of these systems as a function of neutralization and polymer concentration is essential to evaluate the ability of carbopol polymers to jellify for a range of pH values and their potential use as dermatological bases.

The aim of the present study was to assess the rheological behavior of SLN-based semisolid formulations prepared with Carbopol®940 as jellifying agent. To gain some insight into the influence of storage temperature and nature of lipid matrix, the shear stress variation was recorded at a pre-defined shear rate from 0 to 100 s^{-1} for semisolid systems stored at three different temperatures. The rheological properties of carbomer gels have been characterized in several studies (27,28); therefore, they are not reported here. The focus of the present investigation was the rheological behavior of such gels when lipid nanoparticles are entrapped into their network. According to this, analysis has been performed for SLN-based formulations.

The results were recorded after 1 week of storage at 5°C, 25°C, and 40°C and showed pseudoplastic flow behavior at all temperature conditions (Fig. 5) (29). The characteristic concavity of the rheogram toward the shear rate axis indicates that all developed formulations exhibited pseudoplastic flow. This pseudoplasticity results from a colloidal network structure that aligns itself in the direction of shear, thereby decreasing the viscosity as the shear rate increases. SLN-loaded hydrogels showed that up curve does not coincide with the down curve, meaning that the samples also show thixotropy, however with lower structural breakdown.

Ex Vivo Study Using HCS

The *ex vivo* permeation of MN through HCS from MN-SLN gels was evaluated using Franz diffusion cell. The mean cumulative amount diffused Q (mg/cm^2) at each sampling time point was calculated (Fig. 6); high amount of MN release was facilitated through HCS from marketed gel (0.527 mg/cm^2) of MN than the SLN gel (0.289 mg/cm^2). In the present investigation, MN-SLN gel produced significantly higher deposition of MN in skin (57±0.65%) than marketed gel (30%±0.87) as shown in Table III. Nanoparticulate gel shows higher localization of MN in skin as compared to conventional gel (Fig. 7). Thus, drug-localizing effect in the skin seems possible with novel colloidal particulate drug carriers such as SLN. This colloidal carrier, being submicron in size, enhances the drug penetration into the skin, and, because of its lipoidal nature, the penetrated drug concentrates in the skin and remains localized for a longer period of time, thus enabling drug targeting to the skin (18).

CONCLUSION

In conclusion, compritol-888-ATO-based SLN dispersions containing miconazole having low particle size and long-term physical stability are prepared successfully using HPH technique. Lipid content and surfactant play an important role in drug entrapment and particle size. With gel containing nanoparticulate dispersion, a greater quantity of drug remained localized in the skin with lesser amount penetrating into the receptor compartment *ex vivo* as compared with conventional gel, thus enabling drug targeting to skin.

ACKNOWLEDGEMENTS

REFERENCES

1. R. H. Müller, K. Mäder, and S. Gohla. Solid lipid nanoparticles (SLN) for controlled drug delivery—review of the state of the art. *Eur. J. Pharm. Biopharm.* **50**:161–177 (2000).
2. A. Sylvia, R. H. Müller, and S. A. Wissing. Cosmetic applications for solid lipid nanoparticles (SLN). *Int. J. Pharm.* **254**:65–68 (2003).
3. V. Jenning, A. Gysler, M. Schäfer-Korting, and S. H. Gohla. Vitamin A loaded solid lipid nanoparticles for topical use: occlusive properties and drug targeting to the upper skin. *Eur. J. Pharm. Biopharm.* **49**:211–218 (2003).
4. S. A. Wissing, and R. H. Müller. The influence of solid lipid nanoparticles on skin hydration and viscoelasticity—*in vivo* study. *Eur. J. Pharm. Biopharm.* **56**:67–72 (2003).
5. A. ZurMühlen, C. Schwarz, and W. Mehnert. Solid lipid nanoparticles (SLN) for controlled drug delivery—drug release and release mechanism. *Eur. J. Pharm. Biopharm.* **45**:149–155 (1998).
6. S. Utreja, and N. K. Jain. Solid lipid nanoparticles. In N. K. Jain (ed.), *Advances in Controlled and Novel Drug Delivery*, CBS, New Delhi, 2001, pp. 408–425.
7. C. S. Maia, W. Mehnert, and M. Schäfer-Korting. Solid lipid nanoparticles as drug carriers for topical glucocorticoids. *Int. J. Pharm.* **196**:165–167 (2000).
8. R. Sivaramakrishnan, C. Nakamura, W. Mehnert, H. C. Korting, K. D. Kramer, and M. Schäfer-Korting. Glucocorticoid entrapment into lipid carriers—characterization by parelectic spectroscopy and influence on dermal uptake. *J. Control. Release.* **97**:493–502 (2004).
9. S. P. Vyas, and R. K. Kharss. Nanoparticles. In S. P. Vyas, and R. K. Khar (eds.), *Targeted and Controlled Drug Delivery—Novel Carrier Systems*, CBS, New Delhi, 2002, pp. 331–338.
10. R. H. Muller, M. Radtke, and S. A. Wissing. Solid lipid nanoparticles (SLN) and nanostructured lipid carriers (NLC) in cosmetic and dermatological preparations. *Adv. Drug Deliv. Rev.* **54**:S131–S155 (2002).
11. C. Song, and S. Liu. A new healthy sunscreen system for human: solid lipid nanoparticles as carrier for 3, 4, 5-trimethoxybenzoyl-chitin and the improvement by adding vitamin E. *Int. J. Biol. Macromol.* **36**:116–119 (2005).

12. E. B. Souto, S. A. Wissing, C. M. Barbosa, and R. H. Müller. Development of a controlled release formulation based on SLN and NLC for topical clotrimazole delivery. *Int. J. Pharm.* **278**:71–77 (2004).

13. H. B. Chen, X. L. Chang, X. L. Yang, D. R. Du, W. Liu, Y. J. Yang, and H. B. Xu. Podophyllotoxin-loaded solid lipid nanoparticles for epidermal targeting. *J. Control. Release.* **110**:296–306 (2006).

14. V. Venkateswarlu, and K. Manjunath. Preparation, characterization and *in vitro* release kinetics of clozapine solid lipid nanoparticles. *J. Control. Release.* **95**:627–638 (2004).

15. R. H. Müller, W. Mehnert, J. S. Lucks, C. Schwarz, A. Zur Mühlen, H. Weyhers, C. Freitas, and D. Rühl. Solid lipid nanoparticles (SLN)—an alternative colloidal carrier system for controlled drug delivery. *Eur. J. Pharm. Biopharm.* **41**:62–69 (1995).

16. A. Z. Mahmoudabadi, and D. B. Drucker. Effect of amphotericin B, nystatin and miconazole on the polar lipids of *Candida albicans* and *Candida dubliniensis. Indian J. Pharmacol.* **38**:423–426 (2006).

17. B. Patel, H. Shah. Antifungal gel formulations, US patent 5002938. (1991).

18. P. V. Pople, and K. K. Singh. Development and evaluation of topical formulation containing solid lipid nanoparticles of vitamin A. *AAPS PharmSciTech.* **7**(4):article 91 (2006).

19. L. Harivardhan Reddy, and R. S. R. Murthy. Etoposide-loaded nanoparticles made from glyceride lipids: formulation, characterization, *in vitro* drug release, and stability evaluation. *AAPS PharmSciTech.* **6**(2):E158–E166 (2005).

20. O. Glatter, and K. Gruber. Indirect transformation in reciprocal space: desmearing of small-angle scattering data from partially ordered systems. *J. Appl. Cryst.* **26**:512–518 (1993).

21. A. Martin. Rheology. In A. E. Martin (ed.), *Physical Pharmacy*, Fourth edn., Lea and Febiger, Philadelphia, 1993, pp. 453–476.

22. R. Barreiro-Iglesias, C. Alvarez-Lorenzo, and A. Concheiro. Poly(acrylic acid) microgels (carbopol®934)/surfactant interactions in aqueous media Part I: nonionic surfactants. *Int. J. Pharm.* **258**:165–177 (2003).

23. Y. L. Yeow, D. Chandra, A. A. Sardjono, H. Wijaya, Y.-K. Leong, and A. Khan. A general method for obtaining shear stress and normal stress functions from parallel disk rheometry data. *Rheol. Acta.* **44**:270–277 (2005).

24. S. Tamburic, and D. Q. M. Craig. Rheological evaluation of polyacrylic acid hydrogels. *Pharm. Sci.* **1**:107–109 (1995).

25. M. J. C. Fresno, A. D. Ramirez, and M. M. Jimenez. Systematic study of the flow behaviour and mechanical properties of Carbopol (R) Ultrez (TM) 10 hydroalcoholic gels. *Eur. J. Pharm. Biopharm.* **54**:329–335 (2002).

26. J. S. Chu, D. M. Yu, G. L. Amidon, N. D. Weiner, and A. H. Goldber. Viscoelastic properties of polyacrylic acid gels in mixed solvents. *Pharm. Res.* **9**:1659–1663 (1992).

27. B. W. Barry, and M. C. Meyer. The rheological properties of carbopol gels. I. Continuous shear and creep properties of carbopol gels. *Int. J. Pharm.* **2**:1–25 (1979).

28. B. W. Barry, and M.C. Meyer. The rheological properties of carbopol gels. II. Oscillatory properties of carbopol gels. *Int. J. Pharm.* **2**:27–40 (1979).

29. A. Lippacher, R. H. Muller, and K. Mader. Preparation of semisolid drug carriers for topical application based on solid lipid nanoparticles. *Int. J. Pharm.* **214**:9–12 (2001).